International Immunopharmacology 73 (2019) 581–589

Contents lists available at ScienceDirect

International Immunopharmacology

journal homepage: www.elsevier.com/locate/intimp

Differential effects of inhaled *R*- and *S*-terbutaline in ovalbumin-induced asthmatic mice

Huimin Beng[a], Hao Su[a], Shanping Wang[a], Yihe Kuai[b], Junhua Hu[b], Rui Zhang[b], Fei Liu[b], Wen Tan[b,*]

[a] School of Biology and Biological Engineering, South China University of Technology, Guangzhou 510006, China
[b] Institute of Biomedical & Pharmaceutical Sciences, Guangdong University of Technology, Guangzhou 510006, China

ARTICLE INFO

Keywords:
Terbutaline
Asthma
Ovalbumin
Inhalation
Airway hyperresponsiveness
NF-κB

ABSTRACT

Inhaled terbutaline is commercially available β_2-agonist which consists of equivalent amount of *R*- and *S*-enantiomer. In this study, we aimed to investigate the effects of single enantiomers of terbutaline and its racemate in an ovalbumin (OVA)-induced mouse model of asthma *via.* seven days inhalation and the potential mechanisms involved. In a standard experimental asthma model, BALB/c mice were sensitized and challenged with OVA. *R*-terbutaline (*R*-ter), *S*-terbutaline (*S*-ter) or racemic terbutaline (*rac*-ter) was given *via.* nose-only inhalation for one week. Airway responsiveness to methacholine was measured by the plethysmography in conscious mice. Eosinophils counts in blood and bronchoalveolar (BAL) fluid were determined. The OVA-sIgE in plasma and inflammatory cytokines and mediators in BAL fluid or lung tissue were analyzed by ELISA, qRT-PCR or western blotting. Airway inflammation and remodeling were evaluated with hematoxylin and eosin (HE), periodic acid-Schiff (PAS), and Masson staining. Drug distribution and deposition after inhalation were determined by LC-MS/MS. Our data showed that *R*-ter efficiently ameliorated asthma responses, including airway hyperresponsiveness, eosinophils influx and IL-5 in BALF, plasma OVA-sIgE and significantly reduced pulmonary inflammation, peribronchial smooth muscle layer thickness, goblet cell hyperplasia, and deposition of collagen fibers, as well as downregulation of p38 MAPK phosphorylation and NF-κB expression. Racemic mixture exhibited diminished effects while *S*-ter enhanced airway responsiveness to methacholine and exerted pro-asthmatic effects.

1. Introduction

Asthma is one of the most common lung diseases that afflicts an estimated 300 million people of all ages worldwide [1,2]. It is primarily a chronic inflammation of the airways which is characterized by reversible airflow obstruction and intermittent attacks. The pathogenesis of asthma is perplexing and still remains incompletely understood [3,4]. Most frequently, it was recognized as type 2 inflammatory diseases include activation of T helper 2 cells and release cytokines, such as interleukin-4 (IL-4), IL-5 and IL-13; production of immunoglobulin E (IgE) and the activation of multiple effector cells, resulting in epithelial mucus hyperplasia, smooth muscle hypertrophy, enhanced deposition of subepithelial matrix glycoproteins which collectively termed "airway remodeling" [5,6]. In many cases, Eosinophilic inflammation was thought to be a hallmark of asthma and correlated to airway hyperresponsiveness (AHR) and disease severity [7]. Current therapies for the treatment of asthma are still mainly in controlling symptoms, including bronchodilators and inhaled corticosteroids. Short-acting β_2-agonists (SABAs) remain the most effective bronchodilators available for quick relief of asthma symptoms [8]. Despite clear therapeutic benefit, regular β_2-agonists use has several adverse events including decreased efficacy in bronchoprotection and deterioration of asthma control [9]. Therefore, much more attempts are still needed to investigate the mechanisms of these adverse effects and to make an improvement of current β_2-agonists.

Terbutaline is widely used SABA in the clinic for the treatment of asthma. As with most other β_2-agonists, terbutaline has a single asymmetric center and therefore exists a pair of enantiomers. As is

Abbreviations: AHR, airway hyperresponsiveness; SABA, Short-acting β_2-agonist; *R*-ter, *R*-terbutaline; *S*-ter, *S*-terbutaline; *rac*-ter, *rac*-terbutaline; ee, enantiomeric excess; OVA, ovalbumin; IgE, immunoglobulin E; IL, interleukin; MRM, multiple reaction monitoring; NF-κB, nuclear factor κB; ERK, Extracellular signal-Regulated Kinase; MAPK, mitogen-activated protein kinase; GAPDH, glyceraldehyde-3-phosphate dehydrogenase

* Corresponding author at: Institute of Biomedical and Pharmaceutical sciences, Guangdong University of Technology, 100 Waihuan Xi Road, Guangzhou Higher Education Mega Center, Guangdong 510006, China.
E-mail address: went@gdut.edu.cn (W. Tan).

https://doi.org/10.1016/j.intimp.2019.04.036
Received 23 January 2019; Received in revised form 5 April 2019; Accepted 17 April 2019
1567-5769/ © 2019 Elsevier B.V. All rights reserved.

known that two enantiomers of terbutaline are not identical in pharmacological properties since 1972, the therapeutic effect resides mainly in the *R*-enantiomer (eutomer) with little or virtually no adrenoceptor affinity attributed to the *S*-enantiomer (distomer) [10]. However, today practically all pharmaceuticals of terbutaline are used as racemate and the differential effects of enantiopure isomers have been overlooked [11]. More recent finding reported that *S*-terbutaline (*S*-ter) may be involved in the activation of muscarinic receptor which could generate AHR [12]. Nevertheless, Pharmacokinetic data showed that *S*-ter could be eliminated more rapidly than *R*-terbutaline (*R*-ter), thus increased the ratio of eutomer to distomer and thereby might obscure the adverse effect of *S*-ter [13,14]. Accordingly, it is still disputed as to whether racemic terbutaline (*rac*-ter) should be displaced by enantiopure "chiral switch" product (*R*-ter) [15]. Thus, more detailed information should be given to describe the authentic effects of single enantiomers of terbutaline.

We have recently synthesized *R*-ter with high optical purity and chemical purity [16], and then conducted a study on the more accurate effects of terbutaline enantiomers. Herein, in this study, *R*- and *S*-ter with high enantiomeric excess (ee), along with double molar amount of racemic mixture, were employed to be investigated the asthmatic protective effect on an allergic mouse model of asthma *via.* inhalation. Then we evaluated their differential effects on airway inflammation and remodeling and potential mechanisms involved in inflammatory responses have been explored.

2. Materials and methods

2.1. Animals

Male BALB/c mice (n = 50, 6–8 weeks of age), weighing 18–20 g, were purchased from the Laboratory Animal Center of Southern Medical University (Guangzhou, China) and housed in acrylic cages with food and water *ad libitum* under an environmentally controlled condition (room temperature: 25 ± 2 °C, humidity: 60 ± 5%, 12 h dark–light cycle). All experimental procedures were approved by the Animal Ethics Committee of South China University of Technology.

2.2. Mouse allergic asthma model induced by ovalbumin

Mice were sensitized and challenged with ovalbumin (OVA) or normal saline as previously described [17]. Briefly, mice were sensitized by intraperitoneal (i.p.) injection of 0.2 mL of 2% aluminum hydroxide (ALUM) gel containing 10 μg of OVA (Grade V, Sigma-Aldrich) antigen on days 0 and 14. On days 21, 22 and 23, the mice were challenged with 1% OVA in saline (0.01 g/mL) for 20 min *via.* a nebulizer (PARI Turbo boy). On day 26, a 20 min nebulized OVA challenge with 5% OVA in saline (0.05 g/mL) was conducted (see Fig. 1). The control group received 0.2 mL of saline with 2% ALUM administered intraperitoneally on days 0 and 14 before receiving 20 min nebulized normal saline without OVA on days 21, 22, 23 and 26.

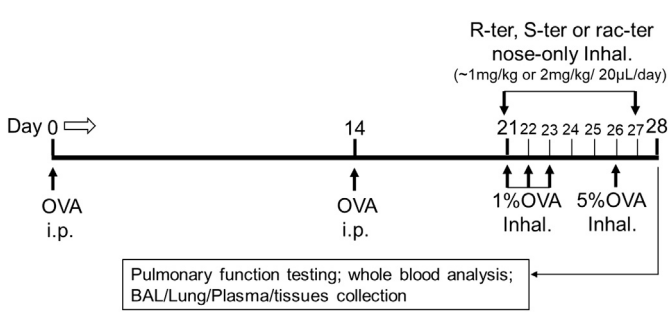

Fig. 1. Study protocol. i.p., Intraperitoneal; inhal., Inhaled; OVA, ovalbumin; BAL, bronchoalveolar lavage.

2.3. Preparation of terbutaline enantiomers and drug dosing

2.3.1. Preparation of R- and S-terbutaline

R-terbutaline (99.9% ee, chemical purity: 99.7%) was obtained by chiral resolution from *rac*-terbutaline (Kangbaotai Pharmaceutical Co., Ltd., Wuhan, China) according to the previously established process [16]. *S*-terbutaline (99.8% ee, chemical purity: 99.6%) was also separated from racemic mixture in a similar procedure as that of *R*-isomer. However, (2*R*, 3*R*)-di-O-(p-toluoyl) tartaric acid (L-DTTA) was used as chiral resolving agent instead of D-DTTA. The detail synthetic protocol and spectroscopic data can be found in the Supplementary data (Scheme S1, Figs. S1 and S2).

2.3.2. Mice nose-only inhalation drug dosing

In three separate experiments (*R*-ter/OVA group, *S*-ter/OVA group and *rac*-ter/OVA group, n = 10), 20 μL of 2 mg/mL *R*-ter or *S*-ter, or double molar amount of *rac*-ter (4.096 mg/mL, all prepared with isotonic saline freshly used) was nebulized by nose-only inhalation tower (Buxco Electronics Inc.). Each 10 mice were then exposed to the corresponding drug aerosol for 5 min on seven consecutive days (day 21–27) before OVA challenge. During exposure, the animals were restrained in the separated chamber and with spontaneous breath. Likewise, for control group (n = 10) and OVA group (n = 10), mice were received normal saline instead for 5 min before challenge.

2.4. Measurement of airway responsiveness to Mch

In vivo airway responsiveness to methacholine (Mch, TCI Development Co., Ltd.) was assessed on day 28 in conscious, freely moving, spontaneously breathing mice by a whole-body plethysmography (Buxco Electronics Inc.). Mice were challenged with aerosolized saline or increasing concentrations of Mch (2, 10, 20 mg/mL) administered by an ultrasonic nebulizer for 2 min. Before Mch challenge, a 20 μL drug aerosol or saline was given to the mice because of the short-acting bronchodilating effect of terbutaline. The degree of bronchoconstriction was expressed as enhanced pause (Penh), a calculated dimensionless value that correlates with the measurement of airway resistance, impedance, and intrapleural pressure. Penh values were recorded and averaged for 4 min after each nebulization challenge.

2.5. Sample collection and whole blood analysis

After Mch responsiveness, mice were anesthetized with 75 mg/kg pentobarbital sodium intraperitoneally. Whole blood was collected for hematology analysis, while part of the blood was then transferred to a heparinized Eppendorf tube, gently mixed and centrifuged under 845 × g at 4 °C for 10 min to isolate plasma specimen for further analysis. Bronchoalveolar lavage (BAL) was performed on the right lung using 0.3 mL of phosphate buffered saline (PBS) for four times. The saline was instilled into the lungs and allowed to equilibrate for at least 30 s before recovery, after centrifugation supernatants were stored at −80 °C for further cytokines analysis while cell pellet was suspended in 0.5 mL PBS and the eosinophils counts were performed using Wright's stain. Then all the organs (liver, right lung lobe, spleen, kidneys, heart, brain) were excised surgically and washed totally with ice-cold PBS to clear the blood and then blotted dry with filter paper. These tissue specimens were then accurately weighted and stored at −80 °C for detecting the drug distribution by LC-MS/MS.

White blood cell (WBC) counts and differential WBC counts were analyzed using a ProCyte Dx Hematology Analyzer (IDEXX Laboratories) in 4 h after blood collection.

2.6. Measurement of OVA-sIgE

OVA-sIgE in plasma was measured using an enzyme-linked immunosorbent assay (ELISA) kit (mlbio, Shanghai, China) following the

manufacturer's specification.

2.7. Analysis of cytokine levels in BAL fluid

BAL fluid samples were analyzed for the concentrations of mouse IL-4 and IL-5 using commercial ELISA kits according to the manufacturer's instructions (R&D Systems, Minneapolis, Minn). IL-13 was assayed in BAL fluid with a mouse IL-13 immunoassay kit (Abcam, Cambridge, UK) following the manufacturer's protocol.

2.8. Lung histopathology

Lung tissue from left lobe was obtained for histopathology and fixed in 10% formalin for 24 h, followed by paraffin-embedded and then were sectioned at 4 μm for routine staining with hematoxylin and eosin (H&E, Solarbio, Beijing, China), or with periodic acid-Schiff (PAS, Solarbio, Beijing, China), or submitted to Masson's trichrome staining (Baso, Zhuhai, China). Images of the stained lung sections were obtained by an Axisplus image-capturing system (Zeiss, Germany) and then a minimum of 3 bronchi (luminal diameter, 150–500 μm) was analyzed permice for various parameters using an image analyzing computer system (IPP) by pathologists blinded to grouping. The histological score, airway smooth muscle thickness, PAS score (goblet cells hyperplasia), and collagen deposition were evaluated by a semi-quantitative scoring method, as previously described [18–20]. Specific scoring criterions were detailedly described in the Supplementary data.

2.9. qRT-PCR

We analyzed the level of NF-κB mRNA in the lung by quantitative real-time PCR analysis. The total RNA was extracted from lung tissue using RNaEXTM Total RNA Isolation Kit (Generay Biotech, Shanghai, China). The quality and quantity of RNA samples were assessed by NanoDrop ND-2000c spectrophotometer (Thermo Fisher Scientific, Inc., Wilmington, DE). Total RNA (1 μg) was reverse transcribed into cDNA using cDNA Reverse Transcription Kit (Vazyme Biotech, Nanjing, China) according to the manufacturer's instruction. Real-time PCR reactions were performed using the 7500 real-time-PCR system (Applied Biosystems, Foster City, California, USA) with AceQ qPCR SYBR Green Master Mix (Vazyme Biotech, Nanjing, China). The primers, set for mouse, were synthesized by Sangon Biotech (Shanghai, China). The sequences are as follows: NF-κB p65 Foward: ATGGCAGACGATGATC CCTAC; Reverse: TGTTGACAGTGGTATTTCTGGTG, β-actin, Forward: CGTTGACATCCGTAAAGACC; Reverse: AACAGTCCGCCTAGAAGCAC. β-actin was used as an internal control to normalize the gene expression. The relative expression level was compared using the $2^{-\Delta Ct(\Delta Ctsample - \Delta Ctcontrol)}$ method [21].

2.10. Western blot analysis

Total Protein from lung tissue was extracted according to the guidelines of manufacturer (Beyotime, China) and the concentrations were determined by BCA assay (Pierce). An equal amount of Protein (30 μg) was separated by SDS-PAGE on a 12% acrylamide gel for electrophoresis and transferred to a polyvinylidene difluoride (PVDF) membrane (Millipore). Membranes were blocked in 5% milk in Tris-buffered saline with 0.1% Tween-20 (TBST) at 4 °C for 1.5 h. Primary antibodies against p38 MAPK (CST#8690.T, 1:1000), p-p38 MAPK (Thr180/Tyr182, CST#4511.T, 1:1000), NF-κB p65 (GeneTex#GTX102090, 1:1000), p-NF-κB p65 (S536, CST#3033.T, 1:1000) and GAPDH (Affinity#AF7021, 1:1000) were added to react with the proteins on the membrane overnight at 4 °C. After the removal of primary antibody, membranes were washed three times with TBST at room temperature and the membrane was incubated with an HRP conjugated goat-anti-rabbit secondary antibody (Thermo, 1:10000 dilution) for 1.5 h. Subsequently, the membrane was rewashed with TBST buffer and bands were visualized using enhanced chemiluminescence (ECL) reagent (Pierce) and analyzed by ImageLab software (Bio-Rad). GAPDH has been used as a standard to ensure the equal amount of protein present in sample among different lanes.

2.11. Tissue distribution of terbutaline after inhalation

An established UPLC-MS/MS method was used to detect the concentrations of terbutaline in plasma and tissues, as previously described [22]. Briefly, one gram of thawed tissue was mixed with 2 mL of normal saline proportionally and homogenized with a tissue grinder (Scientz-48, Ningbo, China). 50 μL of plasma or tissue homogenate was then transferred into another vial and deproteinated with 150 μL mobile phase B (acetonitrile/water = 95/5, *v*/v; 10 mM ammonium acetate, 0.1% formic acid) with 1245.0 pg/mL salbutamol as internal standard (IS). The sample was vortexed for 5 min and the resulting mixture was centrifuged at 18407 × *g* for 10 min at 4 °C, and a 2 μL aliquot of the supernatant was injected into the UPLC–MS/MS for analysis. The chromatographic separation was performed on an ACQUITY UPLC BEH HILIC column (1.7 μm, 100 mm × 2.1 mm i.d.) equipped with an ACQUITY UPLC in-line filter kit (0.2 μm), linked to a Waters Xevo-TQS mass spectrometry using an ESI source. The calibration curve was prepared at concentrations of 82.126, 164.253, 205.316, 410.633, 821.266, 1642.531, 2053.164, 4106.328 pg/mL for *rac*-terbutaline, while quality control (QC) samples were prepared at the concentrations of 98.552, 657.012, 2463.797 pg/mL for all the three analytes. The calibration curve along with QC samples were injected and assayed in each run of biosample analysis. The calibration curve was established by plotting the peak area ratios of the analytes to IS (Y-axis) *versus* the nominal concentrations of terbutaline (X-axis) using weighted least-squares linear regression analysis. In plasma, the calibration curve was Y = 1.64e4*X-1.03e5 (weighting: $1/x^2$, R^2 = 0.9985). The UNIFI Scientific Information System was employed for all the data acquisition and calculation, supplied by Waters. Typical MRM chromatograms and calibration curves in different tissues can be found in the Supplementary data (Fig. S3 and Table S1).

2.12. Data analysis and statistics

All data were presented as the means ± SEM unless stated otherwise. Statistical comparisons were made using one-way ANOVA with post Bonferroni multiple comparison tests. $p < 0.05$ was considered as significant. All statistical analyses were performed using Prism 6.0 GraphPad software (GraphPad, San Diego, CA, USA).

3. Results

3.1. Effects of R-, S- and rac-terbutaline on OVA-induced airway hyperresponsiveness

In order to study the effects of single enantiomers of terbutaline and racemic mixture on allergic asthma, OVA-induced mouse model was established and airway reactivity was assessed in response to aerosolized Mch by means of noninvasive *in vivo* plethysmography. As shown in Fig. 2, compared with the control group, the baseline value in OVA group was significantly augmented when exposure to blank saline (0.80 ± 0.12 for OVA group *vs* 0.55 ± 0.08 for Control group), indicating that this protocol could induce a mice model of allergic asthma with airway hyperresponsiveness. *R*-ter and double molar amount of *rac*-ter treatment could significantly reduce the baseline Penh values. However, the baseline airway reactivity after *S*-ter treatment was significantly increased (0.70 ± 0.13) compared with the control group. The specific values of baseline airway reactivity were listed in Supplementary data (Table S2). Moreover, *S*-ter treatment group showed an overt exacerbation of airway hyperreactivity in response to the increased doses of Mch. Whereas treatment of *R*-ter attenuated airway

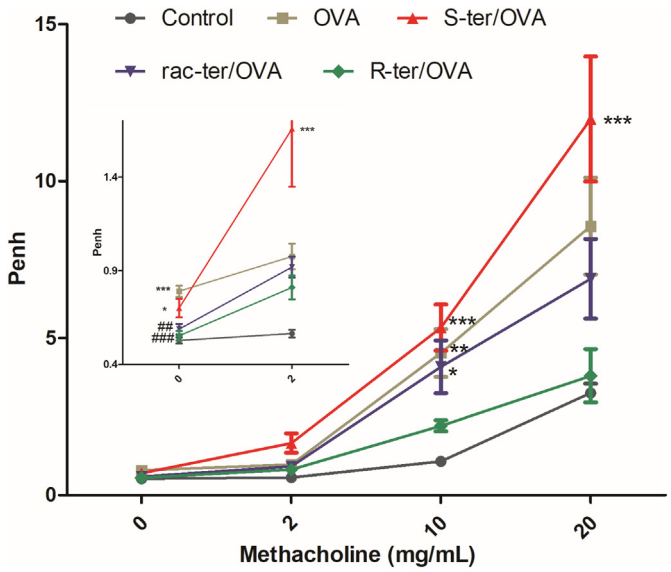

Fig. 2. The degree of bronchoconstriction to aerosolized methacholine (0, 2, 10, 20 mg/mL) after seven days inhalation treatment with *R*-, *S*-, and *rac*-ter in OVA-induced allergic mice. Data is shown as mean ± SEM, (n = 8–10). *p < 0.05, **p < 0.01, ***p < 0.001 *vs* control group. ##p < 0.01, ###p < 0.001 *vs* OVA group.

bronchoconstriction to Mch, suggesting an efficient asthmatic protective effect of *R*-ter. While double molar *rac*-ter administration exhibited a diminished bronchoprotective effect against Mch compared with *R*-ter/OVA group, possibly ascribed to the distomer (*S*-ter).

3.2. Whole blood analysis and eosinophils counts in BAL fluid

To investigate the effects of terbutaline enantiomers on the infiltration of inflammatory cells, Total WBCs and differential WBCs (Neutrophilis, lymphocytes, monocytes, eosinophils and basophils) in blood and eosinophils counts in BAL fluid were detected. As shown in Fig. 3A, total WBCs in blood were similar without significant difference. The percentage of differential WBCs in blood were found to be no significant difference within all the groups besides the percentage of eosinophils counts (Fig. 3B). The EO% in blood was significantly increased in OVA group, *S*-ter treatment and *rac*-ter treatment group when compared with the control group, which are consistent with the results of eosinophils counts in BAL fluid (Fig. 3C). Treatment with *R*-ter significantly inhibited the influx of eosinophils into BAL fluid (Fig. 3C).

3.3. Histopathological evaluation of lung tissue

To further investigate the allergic inflammatory changes in the lung of mice, H&E staining was then conducted. As shown in Fig. 4A, no inflammation, mucosal edema and epithelial lesions were observed in the control group, whereas OVA-induced asthma mice developed severe inflammation, mucosal edema and epithelial lesions, which included interstitial infiltrates and a large number of lymphocyte and eosinophil infiltration. With *R*-ter and double molar *rac*-ter treatment, the degree of inflammatory cell infiltration was ameliorated respectively, which was confirmed by the histological score (Fig. 4B). Meanwhile, OVA-treated mice exhibited an increased thickness of the peribronchial smooth muscle layer, which could suppress by *R*-ter and slightly promote by *S*-ter (Fig. 4C). Similarly, PAS and Masson staining results displayed that the hyperplasia of airway goblet cells (Fig. 4D) and collagen deposition (Fig. 4E) were significantly increased in the OVA group, which markedly reversed after *R*-ter treatment.

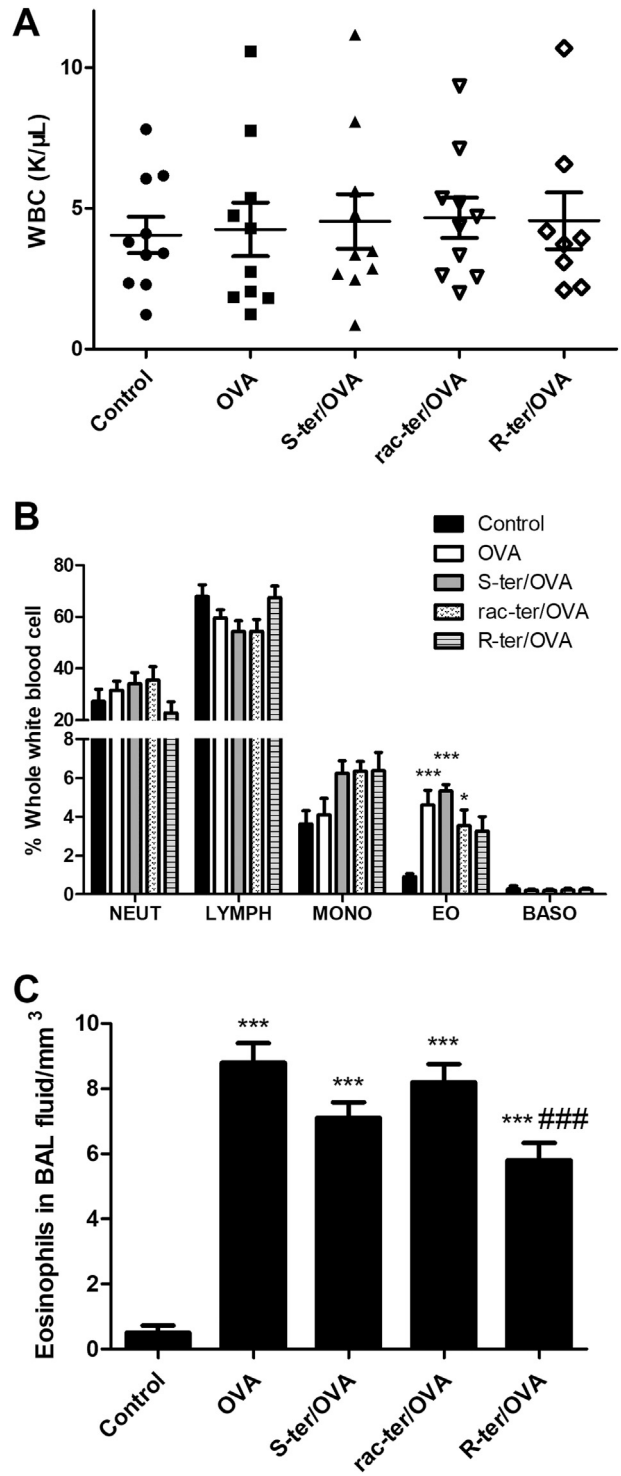

Fig. 3. Whole blood analysis using IDEXX Procyte Dx and eosinophils counts in BALF using Wright's staining. (A) White blood cell (WBC) counts; (B) Differential WBC counts; (C) Eosinophils counts in BALF. Data is shown as mean ± SEM, (n = 8–10). *p < 0.05, ***p < 0.001 *vs* control group. ###p < 0.001 *vs* OVA group.

3.4. OVA-sIgE and Th2 cytokines measurements

Asthmatic inflammation is well known to be initiated by the secretion of series of pro-inflammatory mediators. We assessed OVA-sIgE in plasma and representative Th2 cytokines (IL-4, IL-5, IL-13) in BAL fluid. Mice treated with OVA displayed a significant increase in OVA-

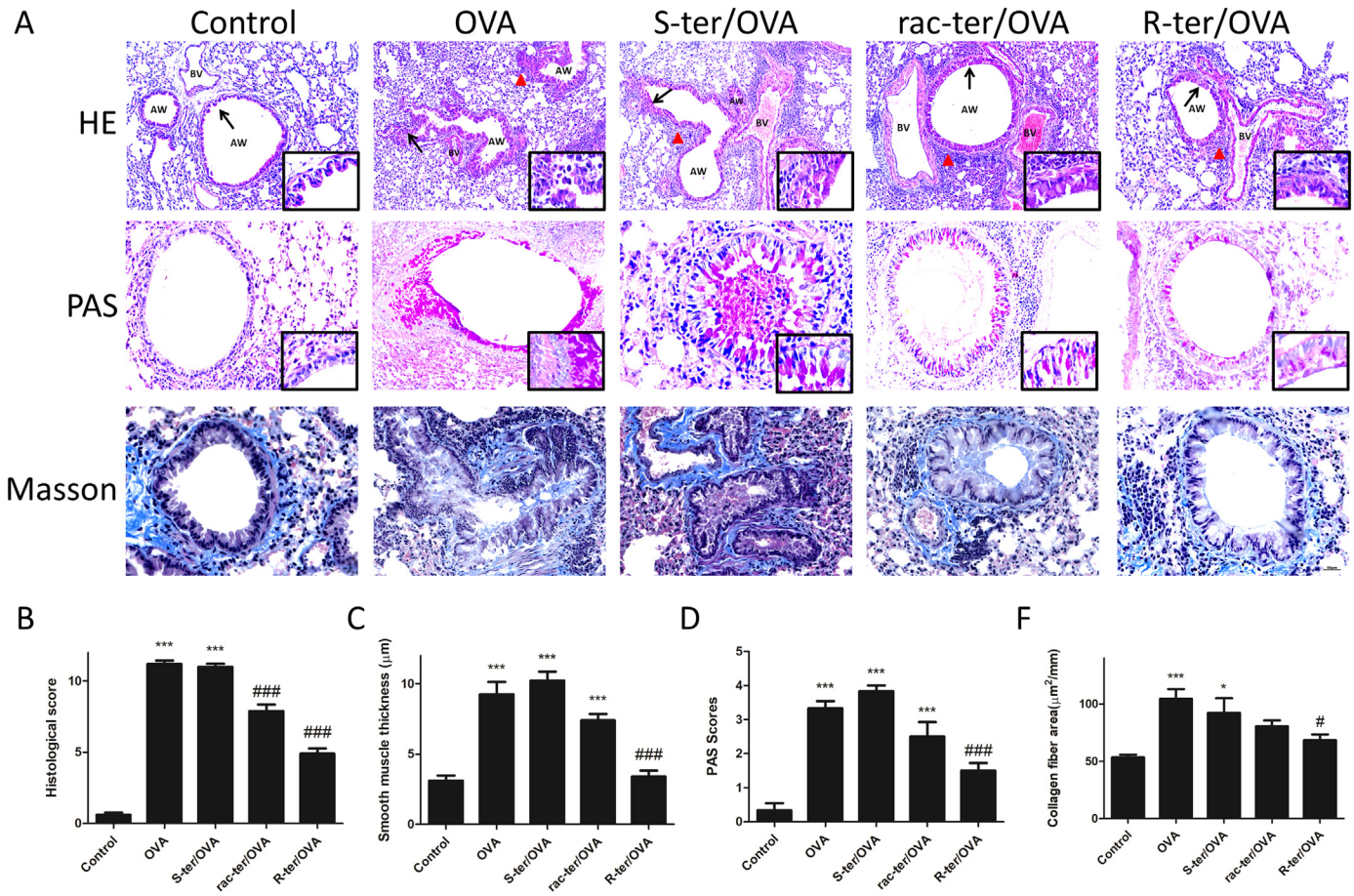

Fig. 4. Effects on lung histopathologic changes after seven days inhalation treatment with *R*-, *S*- and *rac*-ter in OVA-induced allergic mice. BALB/c mice were sensitized and challenged with OVA as described in "Materials and methods". Left lung tissues were obtained on day 28 and stained with hematoxylin and eosin (H& E), periodic acid-Schiff (PAS) or Masson's stain (A) (magnification: ×400). (B) Lung histological score, Statistical data is shown as mean ± SEM, (n = 8–10); (C) Airway smooth muscle thickness, (n = 8–10); (D) PAS scores, (*n* = 6); (E) Lung collagen fiber deposition, (n = 6). Black Arrows indicate zooming site, red arrowheads indicate eosinophils and other inflammatory cells. AW, Airway; BV, blood vessel. Bars = 50 mm. *p < 0.05, ***p < 0.001 *vs* control group. #p < 0.05, ###p < 0.001 *vs* OVA group. (For interpretation of the references to colour in this figure legend, the reader is referred to the web version of this article.)

sIgE level, while markedly inhibited by administration of *R*-ter (Fig. 5A). Likewise, Th2 cytokines (IL-4, 5 and 13) were found to be augmented in OVA-treated group, but without significant difference in IL-4 and 13 expressions. Nonetheless, *R*-ter-treated mice showed a reduced release of IL-4 and IL-13, and significantly decreased the BAL fluid level of IL-5 (Fig. 5B, C, D). Of note, *S*-ter could activate the expression of IL-4 and IL-13 (Fig. 5C, D).

3.5. Drug distribution in tissues after seven-days inhalation

Pulmonary delivery administration, which acts topically in the lung, can offer a direct way to investigate the effect of a compound against asthma. The therapeutic effect of aerosolized drugs is dependent upon the dose deposited and its distribution within the lung. To verify the distribution of terbutaline dosing by this route, the concentrations of terbutaline in plasma and the main organs of mice were measured. With regard to the different metabolism of terbutaline enantiomers, the concentrations of terbutaline in tissues were calibrated by the corresponding concentrations in plasma. As shown in Fig. 6, a much higher concentration of terbutaline in the lung was observed in each group after inhalation (relative concentration of plasma: *S*-ter, 10.79 ± 4.52; *rac*-ter, 31.96 ± 6.52; *R*-ter, 22.39 ± 1.93). These results indicated that after exposure to the drug aerosol, most of the active drug could reach into the lung and generate the corresponding effect on the site of action. *R*-, *S*- and double molar *rac*-ter were widely distributed in various organs after one-week inhalation, and the highest concentration in each group was observed in the lung, followed by the kidney, spleen, heart, brain and liver (Fig. 6), suggesting that it might be prone to exposure to a high systemic concentration of drug with long-term use of terbutaline and then giving rise to unwanted adverse effects. The distributions of terbutaline were found without significant difference between *rac*-ter and *R*-ter group except in liver, while the concentrations of *S*-ter in tissues were significantly decreased besides in heart and liver When compared with *rac*-ter group, indicating that *S*-ter had a greater elimination behavior *in vivo* than its counterpart *R*-ter and *R*-ter governed the absorption and distribution properties of *rac*-ter.

3.6. R-terbutaline inhibited p38 MAPK phosphorylation and NF-κB expression in lung tissue by OVA

With a higher concentration of active drug targeted in the lung, it will help us to reveal the authentic effect of single enantiomer of terbutaline. We next investigated the underlying mechanisms of single enantiomers involved in OVA-induced airway inflammation. Activation of NF-κB signaling pathway in asthma induces airway inflammation and AHR, which is an essential role in allergic diseases [23–25]. Upon interaction with OVA, the expression of inflammatory NF-κB was increased in mRNA transcript when compared with the control group (Fig. 7B). As shown in the figure, *R*-ter treatment effectively depressed the elevated NF-κB expression whereas a tendency toward enhanced NF-κB mRNA transcript was observed in *S*-ter-treated group. Similar results have been seen in the phosphorylation of p65 subunit of NF-κB

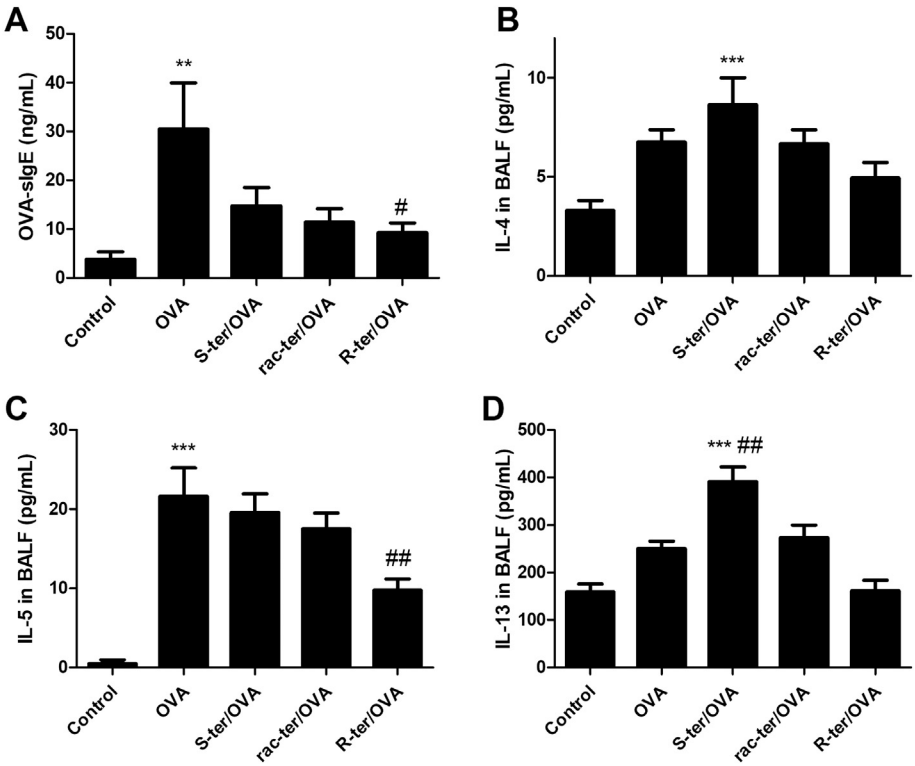

Fig. 5. Effects on the increased levels of OVA-sIgE and Th2 cytokines release after seven days inhalation treatment with *R*-, *S*- and *rac*-ter in OVA-induced allergic mice. (A) OVA-sIgE in plasma; (B) Interleukin (IL)-4 in BALF; (C) IL-5 in BALF; (D) IL-13 in BALF. Data is shown as mean ± SEM, (n = 8–10). *p < 0.05, **p < 0.01, ***p < 0.001 *vs* control group. #p < 0.05, ##p < 0.01 *vs* OVA group.

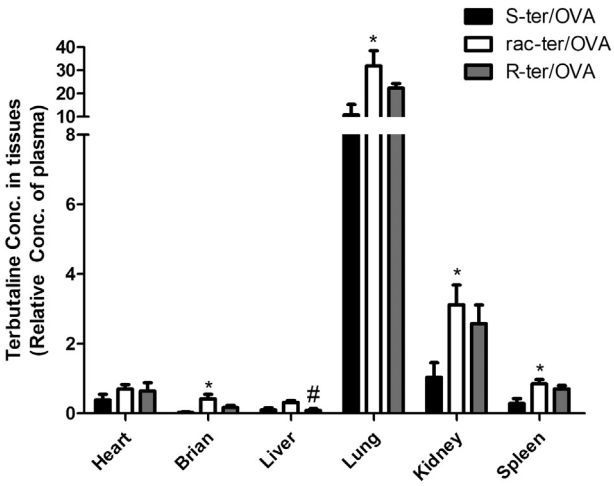

Fig. 6. Terbutaline concentrations in tissues after seven days inhalation treatment with *R*-, *S*-, and *rac*-ter in OVA-induced allergic mice on day 28. Tissues were obtained and terbutaline concentrations were measured by Waters TQS mass spectrometer with a validated method. The concentrations of terbutaline in tissues were calibrated by the corresponding concentrations of terbutaline in plasma. Data is shown as mean ± SEM (n = 8–10). *p < 0.05 *vs* *S*-ter/OVA group. #p < 0.05 *vs* *rac*-ter/OVA group.

(Fig. 7D). MAPKs, especially p38 and ERK1/2, are involved in airway inflammation and regulation of the inflammatory mediators, such as the activation of NF-κB [26,27]. Therefore, we investigated whether the inhibition of inflammatory response by *R*-ter was mediated through MAPKs pathway in OVA-induced asthmatic mice. As shown in Fig. 7C, OVA-treated mice showed markedly upregulated p38 MAPK phosphorylation and significantly suppressed by *R*-ter. Conversely, *S*-ter exhibited an increased p38 MAPK activation as compared with OVA group, albeit no statistically difference. However, the phosphorylation of ERK1/2 was not altered both in OVA and terbutaline-treated group (Data not shown). Collectively, these data revealed that *R*-ter exerted an anti-inflammatory effect on OVA-induced asthmatic mice through inhibiting the activation of p38 MAPK phosphorylation and NF-κB expression. Racemate exerted diminished effects whereas *S*-ter showed a tendency of enhancement of p38 MAPK phosphorylation and significantly promoted the activation of NF-κB in this mouse asthma model.

4. Discussion

Short-acting β_2-agonists, including albuterol and terbutaline, remain the first-line medications in alleviating asthma symptoms due to their ability to promote bronchodilation. However, regular β_2-agonists use has been shown to result in a waning of efficacy, such as decreased bronchodilating effect, increased AHR and cardiac disorders after a high systemic exposure [28–30]. Racemic β_2-agonists, as an equal mixture of *R*-enantiomer and *S*-enantiomer, have raised concerns as to the aforementioned detrimental effects after long term use. *R*-enantiomer of albuterol was reported to exhibit a superiority over racemate based on animal models and some human studies [31–34]. In contrast, *S*-albuterol exerted the opposite effects in comparison with its *R*-enantiomer[35,36]. Terbutaline is an analog of albuterol, which has been found that *R*-ter was 200 times more potent than *S*-ter for β_2-receptor binding [10,37]. However, so far, few researches about the pharmacological effects of terbutaline enantiomers have been published.

In the present study, we utilized a mouse model of allergic asthma induced by OVA to study the differential effects of *R*- and *S*-ter, as well as racemic mixture, *via.* intranasal inhalation for consecutive seven days, and explored the functional mechanisms involved in inflammatory responses. β_2-agonists administered by inhalation enables delivery active drugs targeted to the lung and consequently produces bronchodilating effect [38,39]. Our results showed a higher concentration of active drug deposited in the lung after inhalation (Fig. 6). *R*-ter preferentially retained in the system and appeared to govern the absorption and distribution of racemate. Whereas *S*-ter exhibited a greater elimination behavior *in vivo* than its counterpart *R*-ter. These

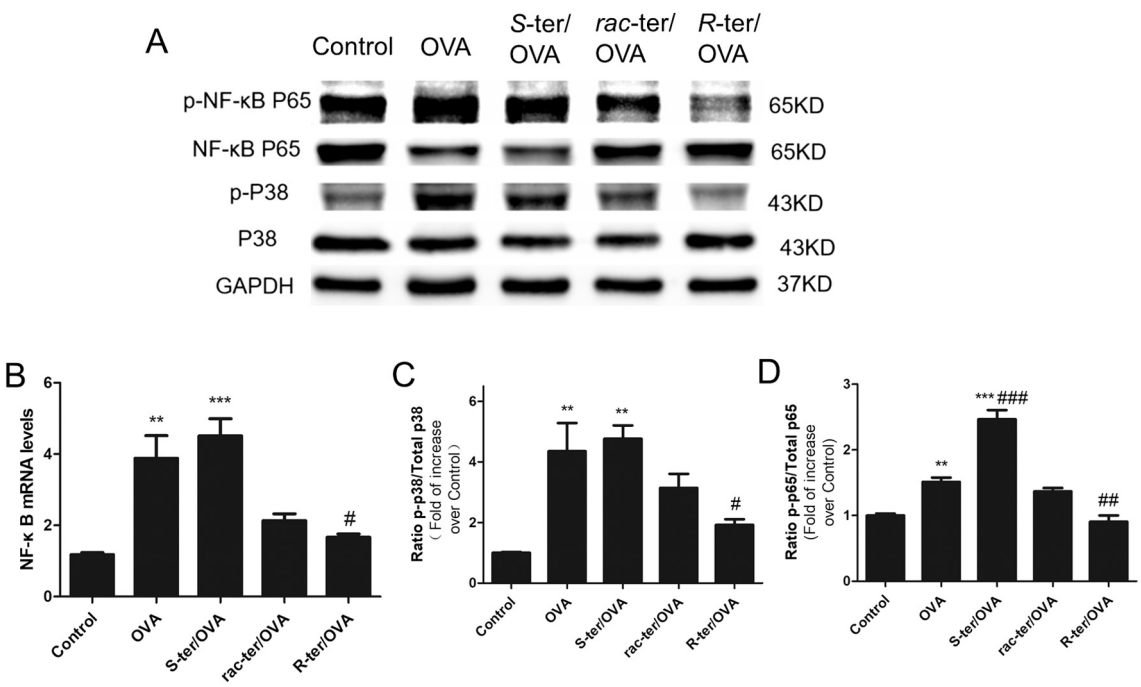

Fig. 7. Effects on p38 MAPK phosphorylation and NF-κB expression in lung tissue after seven days inhalation treatment with *R*-, *S*- and *rac*-ter in OVA-induced allergic mice. (A) Western blot was applied to assess changes in protein expression of p38 MAPK, p-p38 MAPK, p65 and p-p65. GAPDH was used as an internal standard. (B) Results of mRNA expression of NF-κB in lung tissue. Experiments were repeated at least in triplicate ($n = 3$). (C) The p38 MAPK phosphorylation to total p38 MAPK. Values are presented as mean ± SEM. ($n = 4$) (D) The p65 NF-κB phosphorylation to total p65 NF-κB. Values are presented as mean ± SEM. (n = 4). *p < 0.05, **p < 0.01, ***p < 0.001 *vs* control group. #p < 0.05, ##p < 0.01 *vs* OVA group.

results were consistent with the previously published reports on human by L. Borgström [13,14]. Additionally, it was found that the differential metabolic properties of terbutaline enantiomers were interestingly opposite to that of albuterol reported in the early researches [40,41]. Evidence suggests that the majority of β_2-agonists is eliminated *via.* kidney in an unchanged form [11]. In our results, high concentrations of terbutaline in the kidney were observed (Fig. 6). The concentration of *S*-ter in heart was similar to both *R*-ter and racemate, indicating *S*-ter might be prone to accumulate in heart which should be taken concerns in its cardiac effects.

AHR is a key feature of allergic asthma. We found that daily treatment with *R*-ter and racemate *via.* inhalation throughout the antigen challenge phase significantly decreased the baseline airway reactivity and attenuated airway hyperresponsiveness to the inhalation of Mch aerosol. While *S*-ter showed an increased exacerbation of airway hyperresponsiveness at different doses of methacholine when compared with OVA group (Fig. 2). Moreover, double molar *rac*-ter administration exhibited a diminished bronchoprotective effect against Mch compared with *R*-ter/OVA group, possibly ascribed to the counteracting effect of *S*-ter. Similar findings report that *S*-albuterol also shows exaggerated bronchial hyperresponsiveness to stimulus (Mch, OVA and histamine) in various experimental animal models [31]. Increases in intracellular calcium ions might provide a mechanistic explanation for the airway hypersensitization induced by *S*-isomer of β_2-agonists [35,36].

Eosinophilic inflammation is a hallmark of asthma and correlates to AHR and disease severity. Under basal conditions, eosinophils predominantly reside in tissues and in the bone marrow. In response to inflammatory stimuli, the equilibrium shifts, and increased numbers of eosinophils are observed migrating in the blood to the site of infection [42]. Studies have demonstrated blood eosinophil count can serve as a predictive biomarker of asthma severity [43]. We found that in this mouse asthma model, a significantly augment eosinophilia in blood was observed in OVA-treated mice, *S*-ter displayed a tendency of increased eosinophilia in blood (Fig. 3B). In consistant with Henderson's result, only *R*-ter was found to significantly reduced eosinophils influx into BAL fluid (Fig. 3C). Many findings suggest that the Th2 cytokine IL-5 is a well-known cytokine and critical for the development, mobilization, survival and degranulation of eosinophils [44,45]. IL-4 and IL-13 might be also related with pulmonary eosinophilia through affecting the eosinophil chemotaxis, like CCL11 [46]. As shown in Fig. 5, BAL fluid level of IL-5 was significantly reduced by *R*-ter which correlated with the decreased eosinophil influx into BAL fluid. Conversely, *S*-ter showed increased levels of IL-4 and IL-13 in BAL fluid. In this regard, Henderson et al., found that *R*-albuterol significantly reduced BAL fluid level of IL-4, not IL-5 and IL-13, and *S*-albuterol had a trend toward the reduction of IL-4 [34]. This implies the effects of *R*- and *S*-ter on Th2 cytokines in BAL fluid might be different from that of albuterol enantiomers. In addition, previous studies suggest that IL-4 and IL-13 have potent effects on mucus secretion [47,48]. In our results, the enhancement of increased IL-4 and IL-13 levels in BAL fluid by *S*-ter could result in mucus hypersecretion in the bronchi of the lung which can be seen in the histopathological data (PAS scores, Fig. 4D). Moreover, in Zhu's research, IL-13 was partially TGF-β1-independent which might lead to tissue remodeling [49]. Therefore, *S*-ter showed aggravated mucus hypersecretion and increased smooth muscle thickness in this mouse model might through IL-4/IL-13 signaling.

As shown in Fig. 5A, both *R*- and *S*-ter reduced OVA-sIgE levels in plasma, but only reduction by *R*-ter reaches statistic significant. The effects of terbutaline enantiomers on the level of OVA-sIgE in OVA-induced mice were consistent with that of albuterol enantiomers in Henderson's study. In their study, both *R*- and *S*-albuterol may decrease allergen-induced pulmonary inflammation. However, we found that *S*-ter showed no protection against OVA-induced airway inflammation. While only *R*-ter efficiently inhibited airway inflammation and airway remodeling induced by OVA (Fig. 4). MAPKs, especially p38 and ERK1/2, are involved in airway inflammation and regulation of the inflammatory mediators, such as the activation of NF-κB [26,27]. NF-κB regulates the expression of a wide range of genes involved in immune-inflammatory responses, thus plays an important role in the

pathogenesis of asthma [23–25]. In Keränen's study, the anti-inflammatory effects of both racemic albuterol and terbutaline are mediated by MKP-1 expression and then inhibited p38 MAPK phosphorylation [50]. We next proceeded to test whether the inhibition of inflammatory responses by *R*-ter was mediated through MAPKs/NF-κB pathway in OVA-induced asthmatic mice. As shown in Fig. 7, *R*-ter efficiently inhibited OVA-induced phosphorylation of p38 MAPK and the expression of NF-κB. Meanwhile, racemic mixture exerted an intermediate inhibition effect. Whereas *S*-ter showed an enhancement of p38 MAPK phosphorylation and significantly promoted NF-κB phosphorylation. Consistent with our results, Ferrada's reported that *R*-albuterol decreases NF-κB activity and exhibits anti-inflammatory effects in activated T cells [51]. Furthermore, in Agrawal's study, *S*-albuterol activates NF-κB pathway, exerting a pro-inflammatory effect on human bronchial smooth muscle cells [36]. As stated above, we can confirm that *R*-ter efficiently inhibits pulmonary inflammation through a pathways involving suppression of p38 MAPK phosphorylation and NF-κB expression. While *S*-ter is found to markedly increase the activity of NF-κB transcription factor in this mouse asthma model.

Therefore, clinic use of short-acting β_2-agonist racemic terbutaline, as albuterol, may cause unwanted adverse effects. Such adverse effects of *S*-enantiomer of β_2-agonist should be taken full consideration in clinical practice. However, the exact sites of action of *S*-albuterol or *S*-ter is still unclear. Further researches to clarify the detailed action of *S*-ter are needed.

5. Conclusion

In conclusion, in this present study, we demonstrate that the pharmacological effects of racemic terbutaline reside in the *R*-enantiomer. *R*-ter has a much more potent anti-inflammatory effect and alleviation of AHR than racemic mixture. This is partially by effectively inhibition of p38 MAPK phosphorylation and NF-κB expression. In contrast, *S*-ter enhanced airway responsiveness to methacholine and exerts pro-asthmatic effects. The results suggest that a low dose of *R*-ter is a promising alternative medication for the treatment of asthma.

Conflict of interest

The authors declare that there is no conflict of interest associated with this study.

Acknowledgment

This work was supported by the Ministry of Science and Technology of Guangdong Province, China under Grant (2015B010109004).

Appendix A. Supplementary data

Supplementary data to this article can be found online at https://doi.org/10.1016/j.intimp.2019.04.036.

References

[1] S.T. Holgate, The epidemic of allergy and asthma, Nature 402 (6760) (1999) B2 Suppl.
[2] Q. Hamid, M. Tulic, Immunobiology of asthma, Annu. Rev. Physiol. 71 (1) (2009) 489–507.
[3] S.T. Holgate, D.E. Davies, Rethinking the pathogenesis of asthma, Immunity 31 (3) (2009) 362–367.
[4] A. Ray, T.B. Oriss, S.E. Wenzel, Emerging molecular phenotypes of asthma, Am. J. Physiol. Lung Cell. Mol. Physiol. 308 (2) (2014) L130–L140.
[5] R.M. Locksley, Asthma and allergic inflammation, Cell 140 (6) (2010) 777–783.
[6] S. Hall, D.K. Agrawal, Key mediators in the immunopathogenesis of allergic asthma, Int. Immunopharmacol. 23 (1) (2014) 316–329.
[7] K.A. Barry, P. Simon, D.S. Robinson, A role for eosinophils in airway remodelling in asthma, Trends Immunol. 25 (9) (2004) 477–482.
[8] M. Johnson, Beta 2 -adrenoceptors: mechanisms of action of beta 2-agonists, Paediatr. Respir. Rev. 2 (1) (2001) 57–62.
[9] C. Mario, C.P. Page, R. Paola, M.M. Gabriella, β2-agonist therapy in lung disease, Am. J. Respir. Crit. Care Med. 187 (7) (2013) 690–696.
[10] K. Wetterlin, Resolution of terbutaline, a new -sympathomimetic amine, J. Med. Chem. 15 (11) (1972) 1182–1183.
[11] D.W. Boulton, J.P. Fawcett, Enantioselective disposition of albuterol in humans, Clin. Rev. Allergy Immunol. 14 (1) (1996) 115–138.
[12] Z. Fan, W. Lin, N. Lv, Y. Ye, W. Tan, R- and S-terbutaline activate large conductance and Ca 2 + dependent K + (BK Ca) channel through interacting with β 2 and M receptor respectively, Biochim. Biophys. Acta Biomembr. 1858 (11) (2016) 2745–2752.
[13] L. Borgström, L. Nyberg, S. Jönsson, C. Lindberg, J. Paulson, Pharmacokinetic evaluation in man of terbutaline given as separate enantiomers and as the racemate, Br. J. Clin. Pharmacol. 27 (1) (2012) 49–56.
[14] L. Borgström, C.X. Liu, A. Walhagen, Pharmacokinetics of the enantiomers of terbutaline after repeated oral dosing with racemic terbutaline, Chirality 1 (2) (2010) 174–177.
[15] B.L. Källström, J. Sjöberg, B. Waldeck, Steric aspects of formoterol and terbutaline: is there an adverse effect of the distomer on airway smooth muscle function? Chirality 8 (8) (1996) 567–573.
[16] H. Beng, H. Zhang, R. Jayachandra, J. Li, J. Wu, W. Tan, Enantioselective resolution of Rac-terbutaline and evaluation of optically pure R-terbutaline hydrochloride as an efficient anti-asthmatic drug, Chirality 30 (6) (2018) 759–768.
[17] J.E. Phillips, L. Renteria, L. Burns, P. Harris, R. Peng, C.M. Bauer, D. Laine, C.S. Stevenson, Btk inhibitor RN983 delivered by dry powder nose-only aerosol inhalation inhibits bronchoconstriction and pulmonary inflammation in the ovalbumin allergic mouse model of asthma, J. Aerosol Med. Pulm. Drug Deliv. 29 (3) (2016) 233–241.
[18] W. Lin, F. Su, R. Gautam, N. Wang, Y. Zhang, X. Wang, Raf kinase inhibitor protein negatively regulates FcεRI-mediated mast cell activation and allergic response, Proc. Natl. Acad. Sci. U. S. A. 115 (42) (2018) E9859–E9868.
[19] M. Chen, Z. Lv, S. Jiang, The effects of triptolide on airway remodelling and transforming growth factor-β1/Smad signalling pathway in ovalbumin-sensitized mice, Immunology 132 (3) (2011) 376–384.
[20] B.G.J. Dekkers, M. Harm, M. Herman, G. Reinoud, Airway structural components drive airway smooth muscle remodeling in asthma, Proc. Am. Thorac. Soc. 6 (8) (2009) 683–692.
[21] T.D. Schmittgen, K.J. Livak, Analyzing real-time PCR data by the comparative C(T) method, Nat. Protoc. (2008) 1101–1108.
[22] T. Zhou, Q. Cheng, C. Zou, T. Zhao, S. Liu, M. Pistolozzi, E. Tan, L. Xu, W. Tan, Simultaneous determination of bambuterol and its two major metabolites in human plasma by hydrophilic interaction ultra-performance liquid chromatography–tandem mass spectrometry, J. Chromatogr. B Analyt. Technol. Biomed. Life Sci. 967 (967C) (2014) 225–234.
[23] L.A. Hart, V.L. Krishnan, I.M. Adcock, P.J. Barnes, K.F. Chung, Activation and localization of transcription factor, nuclear factor- κ B, in asthma, Am. J. Respir. Crit. Care Med. 158 (5) (1998) 1585–1592.
[24] P.A. Baeuerle, T. Henkel, Function and activation of NF-kappaB in the immune system, Annu. Rev. Immunol. 12 (1) (1994) 141–179.
[25] V. Baud, M. Karin, Signal transduction by tumor necrosis factor and its relatives, Trends Cell Biol. 11 (9) (2001) 372–377.
[26] Y. Liu, E.G. Shepherd, L.D. Nelin, MAPK phosphatases — regulating the immune response, Nat. Rev. Immunol. 7 (3) (2007) 202–212.
[27] R. Alam, M.M. Gorska, Mitogen-activated protein kinase signalling and ERK1/2 bistability in asthma, Clin. Exp. Allergy 41 (2) (2011) 149–159.
[28] R.W. Weber, J.A. Smith, H.S. Nelson, Aerosolized terbutaline in asthmatics: development of subsensitivity with long-term administration, J. Allergy Clin. Immunol. 70 (6) (1982) 417–422.
[29] J.W. de Jong, G.H. Koëter, T.W. van der Mark, D.S. Postma, Effects of cessation of terbutaline treatment on airway obstruction and responsiveness in patients with chronic obstructive pulmonary disease, Thorax 51 (7) (1996) 684–688.
[30] E. Israel, V.M. Chinchilli, J.G. Ford, H.A. Boushey, R. Cherniack, T.J. Craig, A. Deykin, J.K. Fagan, J.V. Fahy, J. Fish, M. Kraft, S.J. Kunselman, S.C. Lazarus, R.F. Lemanske, S.B. Liggett, R.J. Martin, N. Mitra, S.P. Peters, E. Silverman, C.A. Sorkness, S.J. Szefler, M.E. Wechsler, S.T. Weiss, J.M. Drazen, Use of regularly scheduled albuterol treatment in asthma: genotype-stratified, randomised, placebo-controlled cross-over trial, Lancet 364 (9444) (2004) 1505–1512.
[31] B.T. Ameredes, W.J. Calhoun, (R)-albuterol for asthma: pro [a.k.a. (S)-albuterol for asthma: con], Am. J. Respir. Crit. Care Med. 174 (9) (2006) 965–969.
[32] F.J. Westerhof, A.B. Zuidhof, L. Kok, H. Meurs, J. Zaagsma, Effects of salbutamol and enantiomers on allergen-induced asthmatic reactions and airway hyperreactivity, Eur. Respir. J. 25 (5) (2005) 864–872.
[33] B.O. Ibe, A.M. Portugal, J.U. Raj, Levalbuterol inhibits human airway smooth muscle cell proliferation: therapeutic implications in the management of asthma, Int. Arch. Allergy Immunol. 139 (3) (2006) 225–236.
[34] W.R.H. Jr, E.R. Banerjee, E.Y. Chi, Differential effects of (S)- and (R)-enantiomers of albuterol in a mouse asthma model, J. Allergy Clin. Immunol. 116 (2) (2005) 332–340.
[35] S. Mitra, M. Ugur, O. Ugur, H.M. Goodman, J.R. McCullough, H. Yamaguchi, (S)-albuterol increases intracellular free calcium by muscarinic receptor activation and a phospholipase C-dependent mechanism in airway smooth muscle, Mol. Pharmacol. 53 (3) (1998) 347–354.
[36] D.K. Agrawal, A. Krishan, P.W. Kelbe, (S)-albuterol activates pro-constrictory and pro-inflammatory pathways in human bronchial smooth muscle cells, J. Allergy Clin. Immunol. 113 (3) (2004) 503–510.
[37] R.N. Brogden, T.M. Speight, G.S. Avery, Terbutaline: a preliminary report of its pharmacological properties and therapeutic efficacy in asthma, Drugs 6 (5) (1973)

324–332.
[38] J.S. Patton, P.R. Byron, Inhaling medicines: delivering drugs to the body through the lungs, Nat. Rev. Drug Discov. 6 (1) (2007) 67–74.
[39] S.D. Anderson, Repurposing drugs as inhaled therapies in asthma, Adv. Drug Deliv. Rev. 133 (2018) 19–33.
[40] R. Reid, Preferential pulmonary retention of (S)-albuterol after inhalation of racemic albuterol, Am. J. Respir. Crit. Care Med. 160 (4) (1999) 1136–1141.
[41] K. Gumbhir-Shah, D.J. Kellerman, S. Degraw, P. Koch, W.J. Jusko, Pharmacokinetic and pharmacodynamic characteristics and safety of inhaled albuterol enantiomers in healthy volunteers, J. Clin. Pharmacol. 38 (12) (2013) 1096–1106.
[42] L. Simson, P.S. Foster, Chemokine and cytokine cooperativity: eosinophil migration in the asthmatic response, Immunol. Cell Biol. 78 (4) (2000) 415–422.
[43] S.W. Yancey, O.N. Keene, F.C. Albers, H. Ortega, S. Bates, E.R. Bleecker, I. Pavord, Biomarkers for severe eosinophilic asthma, J. Allergy Clin. Immunol. 140 (6) (2017) 1509–1518.
[44] K. Takatsu, H. Nakajima, IL-5 and eosinophilia, Curr. Opin. Immunol. 20 (3) (2008) 288–294.
[45] P.S. Foster, A.W. Mould, M. Yang, J. Mackenzie, J. Mattes, S.P. Hogan, S. Mahalingam, A.N.J. Mckenzie, M.E. Rothenberg, I.G. Young, Elemental signals regulating eosinophil accumulation in the lung, Immunol. Rev. 179 (1) (2010) 173–181.
[46] J. Lv, Y. Xiong, W. Li, X. Cui, X. Cheng, Q. Leng, R. He, IL-37 inhibits IL-4/IL-13-induced CCL11 production and lung eosinophilia in murine allergic asthma, Allergy 73 (8) (2018) 1642–1652.
[47] M.W. Karp, Interleukin-13 in asthma pathogenesis, Curr Allergy Asthma Rep 4 (2) (2004) 123–131.
[48] D.A. Kuperman, R.P. Schleimer, Interleukin-4, interleukin-13, signal transducer and activator of transcription factor 6, and allergic asthma, Curr. Mol. Med. 8 (5) (2008) 384–392.
[49] Z. Zhu, R.J. Homer, Z. Wang, Q. Chen, G.P. Geba, J. Wang, Y. Zhang, J.A. Elias, Pulmonary expression of interleukin-13 causes inflammation, mucus hypersecretion, subepithelial fibrosis, physiologic abnormalities, and eotaxin production, J. Clin. Invest. 103 (6) (1999) 779–788.
[50] T. Keränen, T. Hömmö, M. Hämäläinen, E. Moilanen, R. Korhonen, Anti-inflammatory effects of β2-receptor agonists salbutamol and terbutaline are mediated by MKP-1, PLoS One 11 (2) (2016) e0148144.
[51] M.A. Ferrada, E.L. Gordon, K.Y. Jen, H.Z. He, X. Lu, L.M. Barone, S. Amirifeli, D.L. Perkins, P.W. Finn, (R)-albuterol decreases immune responses: role of activated T cells, Respir. Res. 9 (1) (2008) 3.

Differential effects of inhaled *R*- and *S*-terbutaline in ovalbumin-induced asthmatic mice

Huimin Beng[a], Hao Su[a], Shanping Wang[a], Yihe Kuai[b], Junhua Hu[b], Rui Zhang[b], Fei Liu[b], Wen Tan[b*]

a School of Biology and Biological Engineering, South China University of Technology, Guangzhou, China

b Institute of Biomedical and Pharmaceutical Science, Guangdong University of Technology, Guangzhou, China.

*Corresponding author: Wen Tan, Ph.D. Email: went@gdut.edu.cn

Supplementary Data

Contents:

1.1 Synthesis of *S*-terbutaline hydrochloride S1

1.2 Copies of HPLC chromatograms for the chemical purity and optical purity of *S*-terbutaline S1

1.3 Histological assessments of lung tissue S2

1.4 Copies of typical MRM chromatograms obtained by UPLC-MS/MS S3

1.5 Calibration curves in different tissues S4

1.6 Baseline airway reactivity S4

1.1 Synthesis of *S*-terbutaline hydrochloride

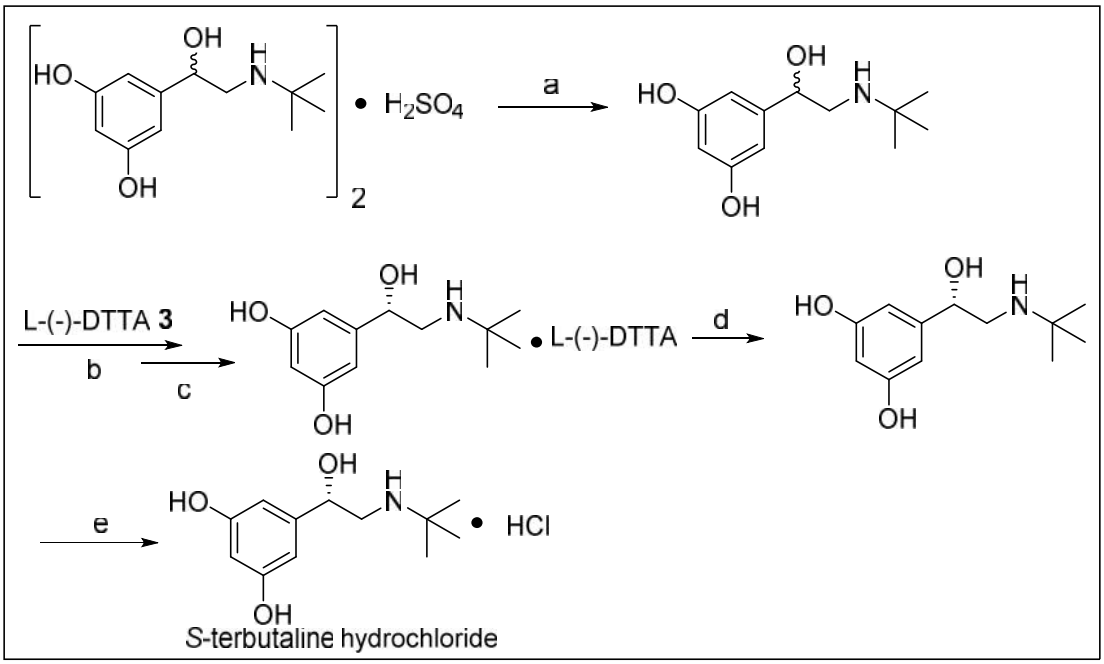

Scheme S1 Synthesis route of *S*-terbutaline hydrochloride. Reagents and conditions: (a) K_2CO_3, MeOH, 70 °C; (b) Acetone, RT; (c) MeOH and DCM, 80 °C (recrystallization 3 times); (d) NaOH, ethyl acetate; (e) ~15–20% ethanolic HCl, 0 °C.

1.2 Copies of HPLC chromatograms for the chemical purity and optical purity of *S*-terbutaline

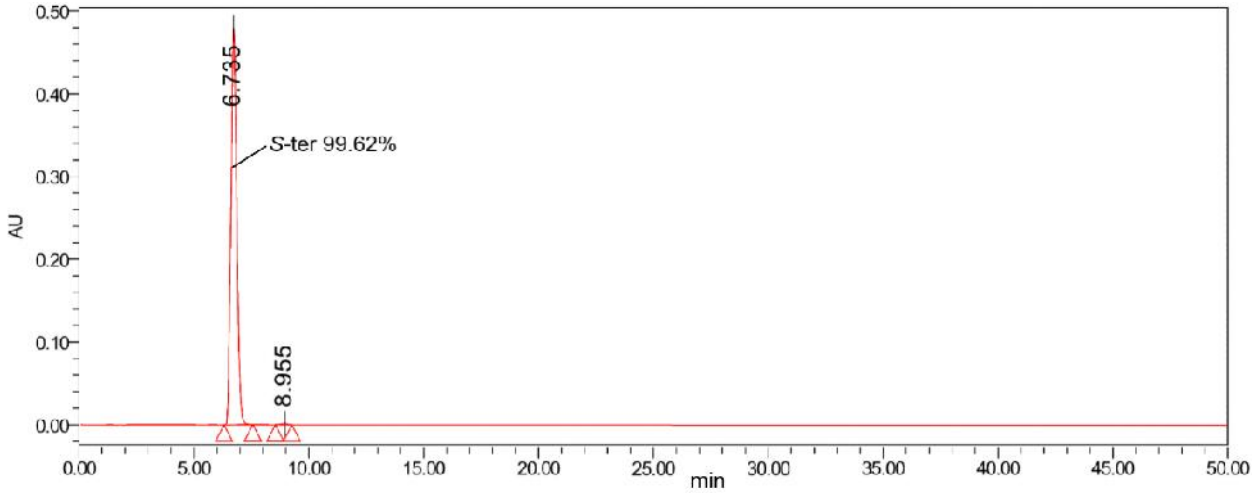

Fig. S1 RP-HPLC chromatogram of *S*-terbutaline. Column: Agilent ODS C18 column (150 mm × 4.6 mm, 5 µm), UV detector: 276 nm. The chemical purity of *S*-terbutaline is signed in the graph.

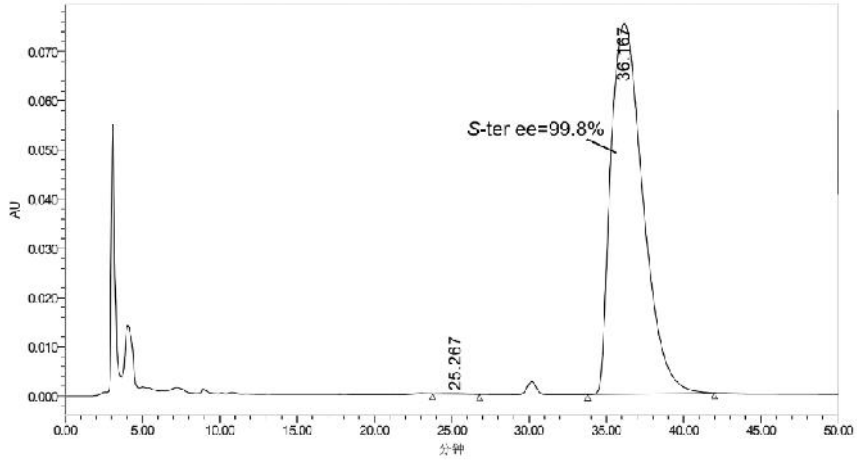

	RT (min)	Peak Type	Area (mAU*sec)	% Area	Height (mAU)	% Height	Integration Type	Peak Codes	Points Across Peak	Start Time (min)
1	25.267	未知	12927	0.12	132	0.18	bb	I08	183	23.750
2	36.167	未知	10863382	99.88	75286	99.82	BB		491	33.800

Fig. S2 NP-HPLC chromatogram of *S*-terbutaline by chiral separation. Column: Daicel CHIRALCEL OJ-H column (250 mm × 4.6 mm, 5 μm), UV detector: 276 nm. The enantiomeric excess (ee) of S-terbutaline is signed in the graph.

1.3 Histological assessment of lung tissue

H&E-stained lung sections were used mainly for the assessment of peribronchial inflammation and airway remodeling, Scores were defined as follows: The infiltration of inflammatory cells was graded 0 for none, 1 for light, 2 for moderate, 3 for severe. The degree of thickening of alveolar septum was graded 0 for none, 1 for light, 2 for moderate, 3 for severe. The desquamation of bronchial epithelial cells was graded 0 for none, 1 for light, 2 for moderate, 3 for severe. For bronchospasm, a value of 0 was none, 1 for light, 2 for moderate, 3 for severe. According to the method, 3 bronchioles with 150–200 μm inner diameter were selected and counted in each slide. The thickness of smooth muscle was measured and the average was calculated. Masson's trichrome-stained sections were used for identification of subepithelial collagen. Briefly, the epithelial basement membranes (diameter ≥ 250 μm) were selected, and the basement membrane perimeter and collagen fiber area (stained in blue) beneath the basement membrane in 20 μm depth were measured. The mean score of the fibrotic area divided by the basement membrane perimeter in every mouse was calculated. PAS-positive area and total area of corresponding bronchial epithelium were calculated, and the adopted grading system was: 0, no goblet cells; 1, <15%; 2, 15–30%; 3, 30–45%; 4, 45–60%; 5, > 60%.

1.4 Copies of typical MRM chromatograms obtained by UPLC-MS/MS

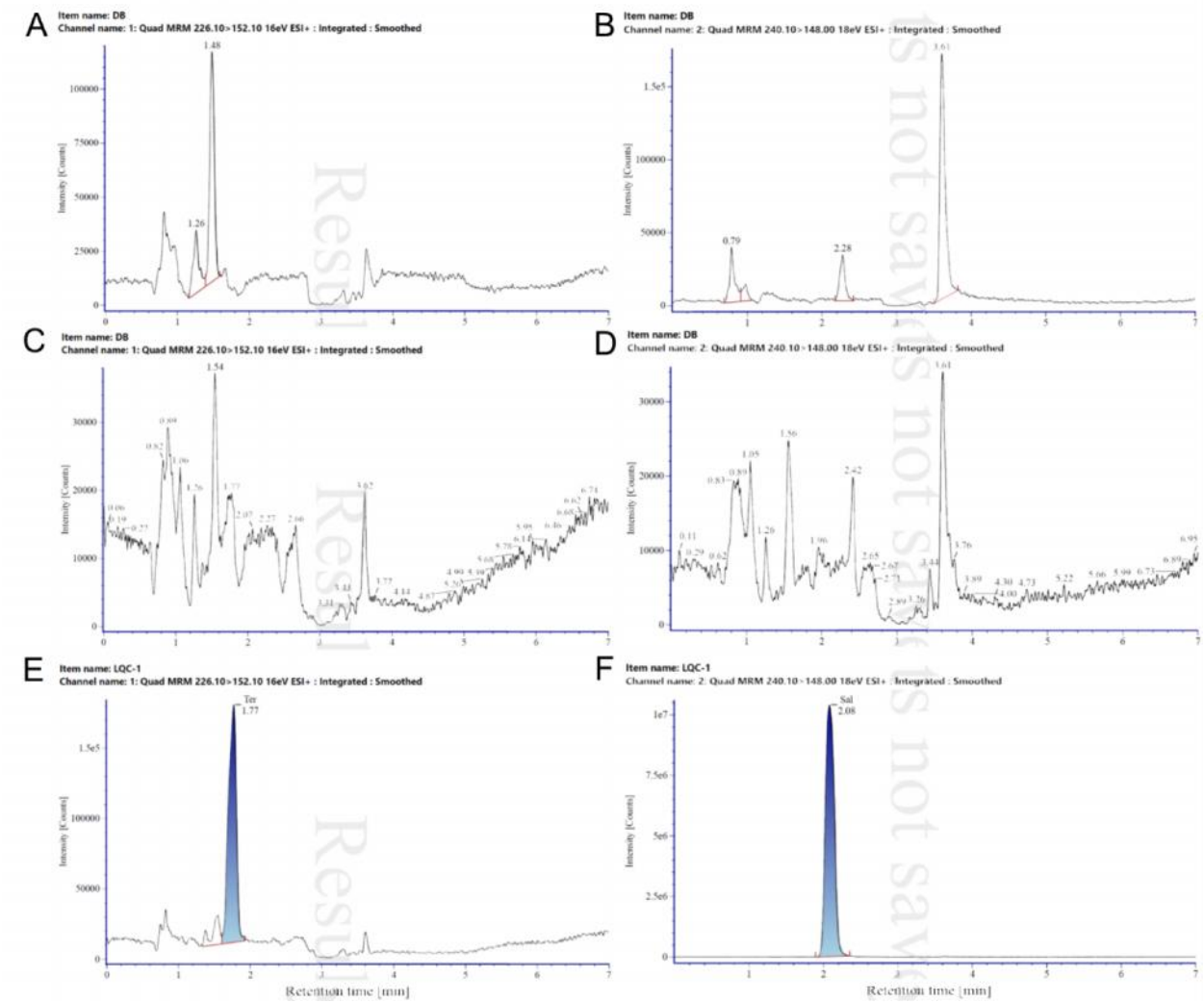

Fig. S3 Typical MRM chromatograms obtained by UPLC-MS/MS. A, Double blank-plasma (MRM:ter); B, Double blank-plasma (MRM:IS); C, Double blank-lung (MRM:ter); D, Double blank-lung (MRM:IS); E, low QC sample-lung (MRM:ter); F, low QC sample-lung (MRM:IS).

1.5 Calibration curves in different tissues

Table S1 Calibration curves, correlation coefficient and %RSD in different tissues

Samples	Calibration curve	Correlation coefficient (R^2)	%RSD
Lung	Y = 1.37e4*X + 5.24e4	0.9977	5.882
Heart	Y = 7.7e3*X + 5.42e5	0.9987	2.901
Liver	Y = 6.74e3*X + 1.32e5	0.9974	5.636
Spleen	Y = 3.7e3*X + 5.31e3	0.9960	7.871
Kidney	Y = 7.36e3*X + 1.63e5	0.9977	5.174
Brain	Y = 8.06e3*X + 5.09e4	0.9967	6.948

1.6 Baseline airway reactivity

Table S2 Baseline airway reactivity when mice were exposure to aerosolized normal saline.

Data is shown as mean ± SD, (n=8-10).

Group	airway reactivity (Penh)	RSD%
Control	0.55±0.08	15.57
OVA	0.80±0.12**	14.79
S-ter/OVA	0.70±0.13*	18.96
RS-ter/OVA	0.59±0.08##	13.58
R-ter/OVA	0.58±0.08###	14.52

**p<0.01, *p<0.05 *vs* control. ##p<0.01, ###p<0.001 *vs* OVA group.